Biology Methods and Protocols, 2026, **11**(1), bpag016
https://doi.org/10.1093/biomethods/bpag016
Published: 26 March 2026
Methods Article

LAMPrey: a standardised method for analysing quantitative LAMP reactions using the inflection cycle threshold

Adam Bates[1], Jiao Li[2], Sofia Vamos[2], Francisco Rivero[3], Katharina C. Wollenberg Valero[2,4,*]

[1]Department of Psychiatry, Warneford Hospital, University of Oxford, Oxford, OX3 7JX, United Kingdom
[2]School of Biology and Environmental Science, University College Dublin, Belfield Campus, Dublin, D04 V1W8, Ireland
[3]Centre for Biomedicine, Hull York Medical School, University of Hull, Hull, HU6 7RX, United Kingdom
[4]Conway Institute, University College Dublin, Belfield Campus, Dublin, D04 V1W8, Ireland

*Corresponding author. School of Biology and Environmental Science, University College Dublin, Belfield Campus, Dublin, D04 V1W8, Ireland. E-mail: katharina.wollenbergvalero@ucd.ie.

Abstract

Quantitative loop-mediated isothermal amplification (qLAMP) is a gene expression quantification method that has gained popularity in recent years, particularly in disease identification, including during the recent SARS-CoV-2 pandemic. Unlike conventional quantitative PCR (qPCR), qLAMP features reaction kinetics that may diverge from sigmoidal expectation, and may not include ROX dye in commercial kits. Determining cycle threshold (Ct or Cq) values through automatic thresholding may therefore produce inaccurate results, and the nature of these thresholds complicates comparability between studies and softwares. We introduce a new method for transforming sigmoidal amplification curves into inflection cycle threshold curves (iCt) to address issues with auto thresholds and analysis of qLAMP. This method is implemented as a set of R functions named *LAMPrey*, suitable for analysis of both qPCR and qLAMP reactions performed in the two most commonly used real-time thermocyclers. We simulate qLAMP amplification differences, demonstrate that iCt and Ct methods perform equivalently for conventional qPCR with an Illumina library quantitation kit, and show that iCt values outperform Ct and the sigmoid curve-fitting metric FDM for quantifying 2416 qLAMP reactions in of zebrafish embryos. All scripts developed for this article are available at https://github.com/dodged13/LAMPrey.

Graphical Abstract

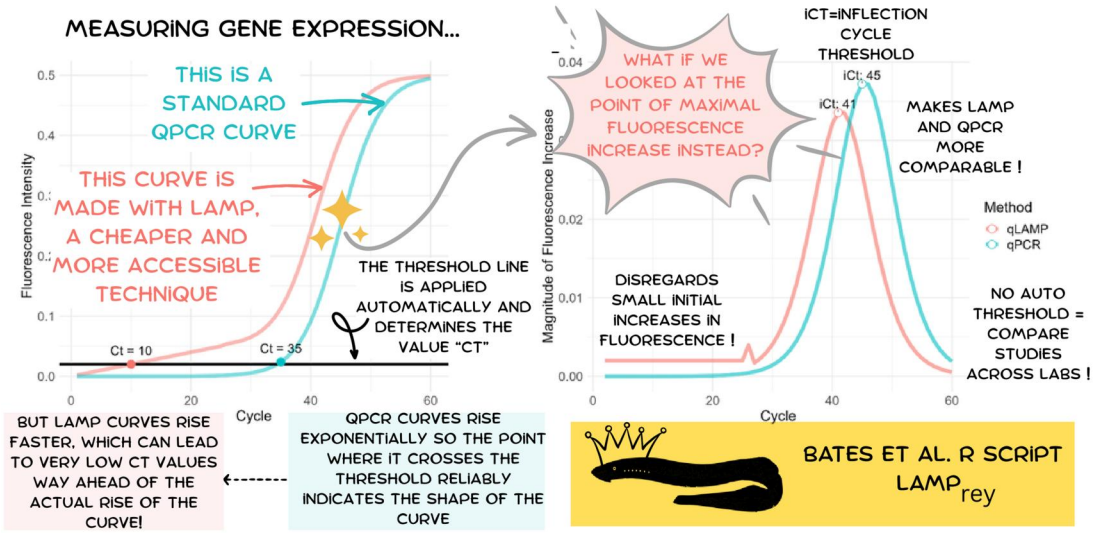

Received: 23 November 2025; **Revised:** 9 March 2026; **Accepted:** 17 March 2026

Keywords quantitative RT-PCR, ddCT, cycle threshold, LAMP

Introduction

Quantifying specific RNA fragments is a fundamental technique in molecular biology and diagnostics, used to analyse RNA derived from organismal tissue, cells, or infectious agents such as viruses. The current gold standard for RNA quantification is quantitative PCR (qPCR or RT-qPCR), framed by the MIQE guidelines in order to standardize the technology and minimize error; this ensures comparability across studies [1]. However, qPCR may not be accessible to all laboratories around the world as it requires a real-time fluorescence detection thermocycler. Loop-mediated isothermal amplification (LAMP) offers a lower-cost alternative for gene expression quantification due to its different chemistry and reaction mechanism [2]. LAMP gained popularity during the SARS-CoV-2 pandemic for its ease of use in detecting viral presence using pH- or turbidity-dependent reporters and therefore removing the requirement for a real-time thermocycler [3, 4]. One study found that LAMP had a detection sensitivity of 87% of SARS-CoV-2 positive cases through a colorimetric readout, with 100% specificity making it a practical option for diagnostic labs with limited access to equipment [5]. Quantitative LAMP (qLAMP) is a method where the fluorescence change of a LAMP reaction is measured. While LAMP can be performed on simple equipment like heating blocks, qLAMP can be performed not only on real-time fluorescence detection thermocyclers but also using plate readers, spectrophotometers, or Qubit machines [6]. This again lowers the accessibility burden. Unlike conventional PCR, LAMP uses four to six primers that create hairpin structures from the template for continuous amplification that are then extended into high molecular weight structures ('handlebars') at constant temperature. RT-LAMP kits contain a reverse transcriptase that allows for the use of RNA as a starting material, eliminating the need for a separate reverse transcription reaction, reducing both time and cost and further increasing the accessibility of the technology. The typical LAMP reaction can provide a result in as quick as 30 minutes, compared to the 45–150 minutes required for conventional PCR methods, however in our experience LAMP reactions can take up to 60 minutes to complete.

For qLAMP performed on thermocyclers, the quantification process is often performed using manufacturer software which typically uses an auto-determined or manually set threshold for calculating cycle threshold (Ct, or alternatively called Cq) values. Here, proprietary algorithms set a threshold during the exponential phase of amplification, which is applied roughly when the fluorescence of the reaction rises above that of the background noise. This dependency on manufacturer-specific software settings reduces transparency and comparability between studies as Ct values are not standardized between laboratories or studies. While relative quantification using reference genes is not affected, this lack of standardization can pose challenges when comparing absolute Ct values, such was observed in the SARS-CoV-2 related quantification of viral load [3]. This approach to Ct calculation also fails to account for variations in reaction efficiency, which can be influenced by contaminants like salts from RNA extraction, leading to inconsistent results between laboratories. Such issues, combined with inadequate laboratory experience or training, contributed to the prevalence of false positive cases during the SARS-CoV-2 pandemic [7]. For qPCR reactions, the MIQE guidelines on best practice emphasise reproducibility but do not specifically address the impact of threshold settings on comparability across studies [1]. In addition, such automatic thresholds can introduce errors when amplification curves deviate from the typical sigmoidal shape of qPCR. qLAMP reactions often exhibit an initial linear phase before entering exponential amplification, which can vary further depending on the template or primers [8]. Therefore, they can deviate from the sigmoidal shape known from qPCR reactions, as was determined in this study. This variability can lead to erroneous early Ct values if the threshold is crossed during the linear phase rather than the exponential phase. An additional possible source of erroneous Ct calls is the fact that commercial LAMP mastermix kits may not include ROX dye, which is used to calculate background fluorescence vs. sample fluorescence (Rn). In the absence of ROX, qPCR thermocyclers may use random background fluorescence for this calculation. Developing transparent and easy to use open-source tools for RNA quantitation, not limited to, but including qLAMP reactions, will enhance reproducibility and foster open science. Here, we present an alternative method to automatic Ct computation based on the starting point of the 5 cycles with maximal fluorescence increase, termed the inflection cycle threshold (iCt). This metric will eliminate problems with (i) the arbitrary nature of threshold values, (ii) the initial linear phase of amplification curves through qLAMP reaction dynamics, and (iii) provide independence from the requirement of ROX background dye. Other methods have been developed for the analysis of qPCR data without the use of threshold and baseline settings, although none of these have been developed specifically for qLAMP. For example, Guescini *et al.* [9], Luu *et al.* [10], and Zhang *et al.* [11] propose to fit a four-point sigmoidal function to qPCR curves and use the first derived maximum (FDM, the midpoint cycle of the function) as the point of maximum fluorescence increase, instead of Ct. FDM is implemented in the LightCycler 480 (Roche) system, and available via the R package *qpcR* [12]. We compare iCt to Ct and FDM using three measures of performance: (i) percentage of successful calls, (ii) deviation between technical replicates, and (iii) overall agreement. The iCt approach enables more consistent quantification, improving the comparability of both qPCR and qLAMP results. We have implemented this method in the set of R scripts termed *LAMPrey*.

Materials and methods

Computing iCt with the *LAMPrey* function

The *LAMPrey* function was developed as follows: the table of raw fluorescence signals per cycle from a real-time thermal cycler—specifically, the GREEN channel for SYBR green reaction chemistry, though it can be adapted for other channels depending on the dye used—was imported into R [13]. While users can modify the input script to fit the template, it can process raw data files produced by two common real-time thermal cyclers, the StepOnePlus real-time thermocycler (Applied Biosystems, MA, USA) and the QuantStudio real-time PCR system (Applied Biosystems). As raw fluorescence signals are not standardized, they are first normalized to themselves by dividing each fluorescence reading at cycle n by the reading at cycle $n + 5$, rather than using a background dye like ROX. These normalized values are plotted as a line graph with cycle number on the x-axis.

A reactivity curve is generated, with the peak of the curve indicating the starting cycle after which the reaction is most active over 5 cycles (~90 seconds of LAMP, roughly corresponding to the length of 1 qPCR cycle), which was recorded as the iCt for downstream analysis. The *LAMPrey* script is available at Supplementary Appendix 1 (https://github.com/dodged13/LAMPrey). For ease of use, *LAMPrey* calculates iCt values and returns them for each sample, as well as being integrated with the R package *ggplot2* [14] to generate publication-ready graphs.

For ease of use, we have also added a *ggplot2* based plotting function called LAMPrey.plot(), which can group the raw data by desired factor by specifying 'Well', 'Task', or 'Gene' (Fig. 1A–C, respectively). As the function uses *ggplot2*, it can be combined with users' already existing themes or overlaid with other graphs or annotations, and can be faceted to give a better overview of the data (Fig. 1D).

Validation of iCt and Ct using qPCR standards of known cDNA concentration

qPCR data was derived from an NEBNext® Illumina library quant kit consisting of a set of standards with known cDNA concentration (New England Biosciences, MA, USA; Cat #E7630S). qPCR reactions were performed as per manufacturers' instructions provided with the kit. Subsequently, both StepOne thermocycler-based Ct and *LAMPrey* iCt values were calculated for the same reactions, to verify that iCt accurately quantifies cDNA of known concentration. The fit of both methods was evaluated with a scatterplot and the coefficient of determination (R^2) obtained via a linear model.

qPCR reactions of known standards

To compare the performance of different metrics in determining the threshold of successful amplification for LAMP data, we amplified 26 genes from total RNA of 24 hours post-fertilization zebrafish (*Danio rerio*) embryos. The primers were designed with the NEB's LAMP primer design tool, using the .fasta sequences of the genes of interest from NCBI's RefSeq database and ordered from IDT (Leuven, Belgium). Primers were selected for having closely related melting temperatures (T_M) as well as allowing 120–180 bp for F1–F2. B1–B2 primers were selected so that spacing would allow loop formation [2] and that loop primers (Loop F and Loop B) could be added to the reaction mix to speed up the reaction. For ease and to reduce pipetting errors, each primer set was combined per gene as a 10× stock and added to each reaction as a mix (Table 1). Warmstart LAMP kits were ordered from New England Biosciences (MA, USA; Cat# E1700).

qLAMP reactions of 24 hpf zebrafish embryos

Across several independent experiments from four researchers (A.B., J.L., S.V., and V.S.), RNA samples were extracted from pooled sets of 20 zebrafish embryos per each sample. Tissue was first homogenized in Trizol™ using a sterile manual pestle. A standard Trizol™ extraction was performed as per manufacturer's instructions (Invitrogen, CA, USA), although modified by the addition of an extra 75% ethanol wash step of the RNA pellet (wash performed as outlined in the manufacturer's protocol) in order to better remove phenol contamination. Quality was assessed using a ND-1000 Nanodrop spectrophotometer (Thermofisher, MA, USA); 70 ng of total RNA has previously been found to be sufficient to generate reliable results from qLAMP [15], and so this was used across all reactions. After initial tests with the 25 μL total reaction volume as suggested by the manufacturer, and a reduced 10 μL reaction volume (Table 2), no differences in effectiveness were detected and 10 μL reactions were subsequently performed. In order to minimise pipetting errors, the fluorescent dye was added to the overall mastermix including primer mix, and LAMP Warmstart mastermix. RNA was mixed with RNase free water and added in last. Freezing the overall mastermix overnight had no negative effect on reactions. The LAMP reaction itself was performed in a

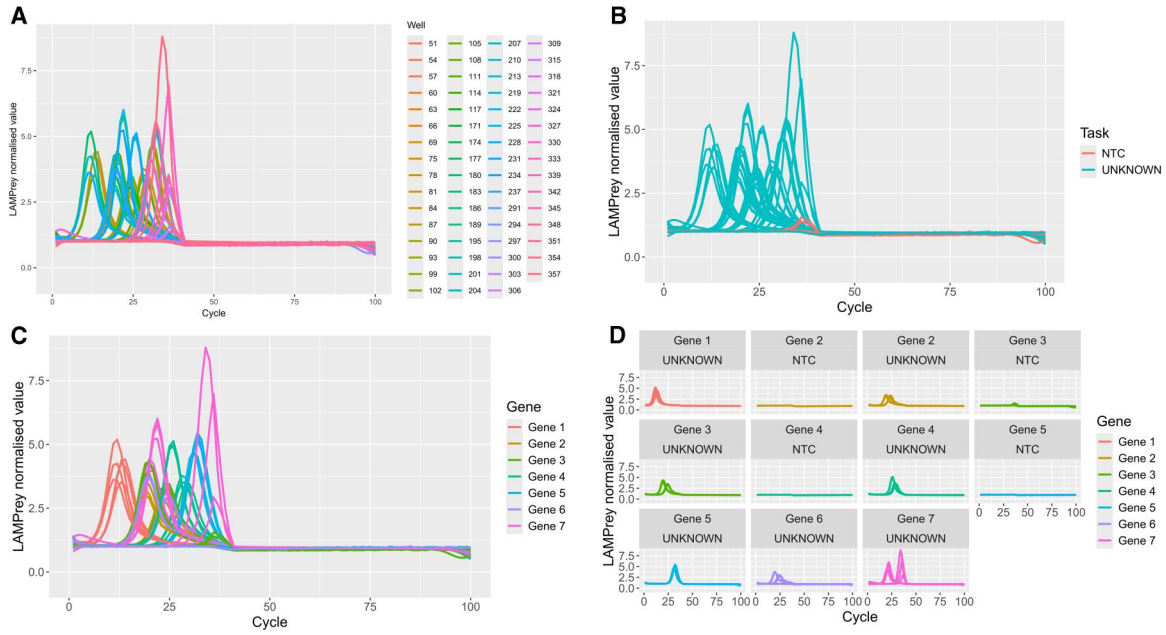

Figure 1 Example outputs of the LAMPrey.plot() function using qPCR data where either A) well, B) task, or C) gene has been defined as the grouping variable. D) is the gene output but facet wrapped by gene and task (NTC = no template control; UNKNOWN = sample of unknown quantity/experimental sample) using ggplot's facet_wrap() function, showing the ability to modify the plot using ggplot2 functions.

StepOnePlus real-time thermocycler (Applied Biosystems) for 100–200 'cycles' of 18 seconds and a reading was taken at the end of each cycle. With these settings, each reaction had a total reaction time of 30–60 minutes, with temperature set at a constant 65°C.

Test of iCt, Ct, and FDM methods on qLAMP data

One dataset (dubbed 'dataset 1', experimenter S.V.) contained 14 genes across 2016 wells amplified with qLAMP. This dataset had an overall higher variability of machine-derived Ct values, and in addition 19 plates had ROX dye added and three had not. Dataset 1 was therefore chosen for in-depth analysis and comparison of methods. FDM and iCt values for all plates were computed in R and added to this dataset (R script is available as Supplementary Appendix 2 and in https://github.com/dodged13/LAMPrey). Additionally, to iCt computed across 5 cycles (in the following called iCt_5), iCt values of 1 and 2 18-second cycles were explored and included in comparisons. Performance of methods was evaluated using (i) percentage of successfully called wells, (ii) deviation between technical replicates, and (iii) overall agreement depicted by Bland-Altman agreement plots. To determine dispersion between technical replicates, median absolute deviation (MAD) describes the median of the absolute differences between each data point and each dataset's median. In this case, 'dataset' is each group of three replicates. In order to not artificially improve the MAD for any metric by removing technical replicate groups with missing values, this parameter was computed on the dataset where 'Undetermined' calls were replaced with the value 200. A Kruskal–Wallis test with *post hoc* Dunn's test was performed to test for differences in MAD among metrics. Bland-Altman agreement plots were created only on paired observations, excluding all datapoints where calling failed in either method, either due to ROX presence vs. absence or to other reasons, and wells with largest disagreement were plotted.

A second dataset (dubbed 'dataset 2') contained 397 qLAMP reaction wells for 14 genes, and about half of the reactions had ROX dye

Table 1 The composition and the concentrations of the LAMP primer mix used in the reactions.

Primer	10× Concentration	Working concentration
FIP	16 µM	1.6 µM
BIP	16 µM	1.6 µM
F3	2 µM	0.2 µM
B3	2 µM	0.2 µM
LOOP F	4 µM	0.4 µM
LOOP B	4 µM	0.4 µM

Table 2 Composition of the 10 µL qLAMP reactions. The reaction can be performed with either RNA or cDNA as the input material.

Component	Supplier (cat #)	Experimental	No template control
WarmStart LAMP 2× Master Mix	NEB (E1700S)	5 µL	5 µL
LAMP Fluorescent Dye (50×)	NEB (B1700SVIAL)	0.2 µL	0.2 µL
ROX (50×) (optional)	Invitrogen (#12223012)	0.2 µL	0.2 µL
LAMP Primer Mix (10×)	IDT	1 µL	1 µL
Target RNA/cDNA	—	70 ng total RNA	—
Nuclease free H_2O	—	Up to 10 µL	Up to 10 µL

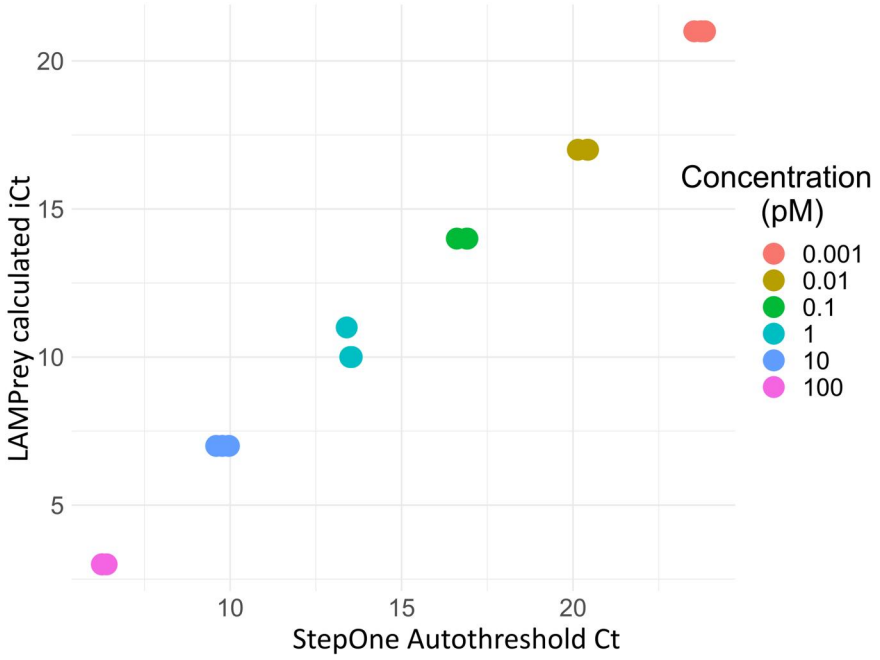

Figure 2 The iCt values calculated for qPCR amplification curves of the standards of a NEBNext quant library kit by iCt_5 compared to the Ct values provided by the StepOne software. The concentration of the standard is listed as pM. Linear modelling calculated the correlation coefficient (R^2) between the two methods to be 0.9967.

added to them (experimenter J.L.), while the other half had not (experimenters A.B. and V.S.). This dataset was used to compare goodness-of-fit as an example of a qLAMP dataset with lower variability in automatically called Ct values.

Results and discussion

LAMPrey iCt was correlated with qPCR Ct when analysing qPCR standards

The comparison between the Ct values generated by the StepOne software and the iCt values from the *LAMPrey* function showed a high correlation, with an R^2 value of 0.99 (Fig. 2). These results show that *LAMPrey* can accurately detect differences in input concentration of

Table 3 Percentage of undetermined wells not called by a metric for plates with ROX dye added vs. plates without ROX dye.

Rox status	Metric	% Undetermined wells
No ROX	Ct	43.73
No ROX	iCt_1	14.34
No ROX	FDM	5.02
No ROX	iCt_2	3.58
No ROX	iCt_5	3.22
ROX added	iCt_1	26.16
ROX added	FDM	11.76
ROX added	Ct	8.55
ROX added	iCt_2	8.49
ROX added	iCt_5	7.23

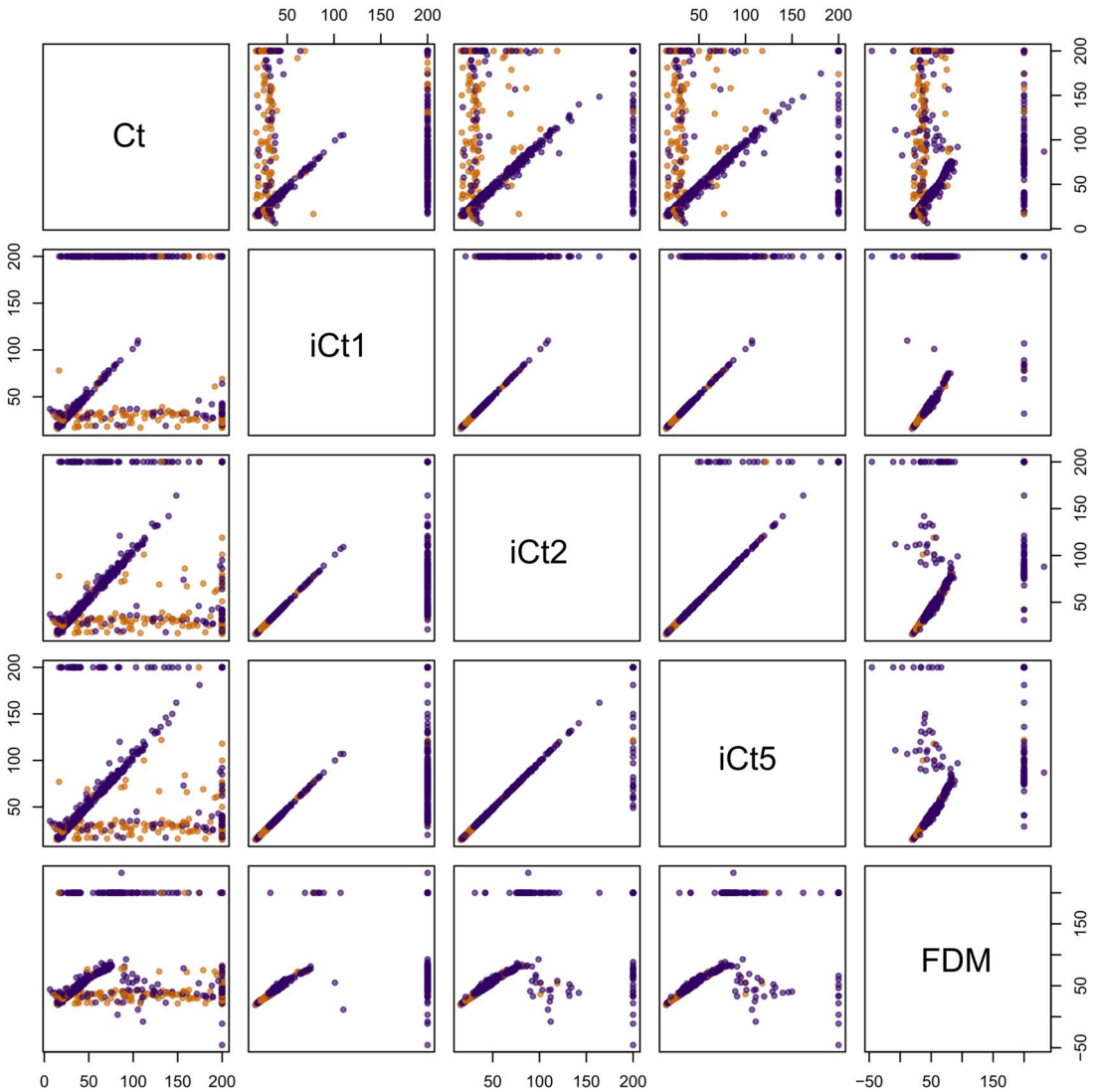

Figure 3 Scatter plot matrix to compare the different metrics quantifying amplification. Ct—cycle threshold method, iCt_1—inflection cycle threshold, averaged over 1 cycle; iCt_2—inflection cycle threshold, averaged over 2 cycles; iCt_5—inflection cycle threshold, averaged over 5 cycles; FDM—first derived maximum of a sigmoidal curve fitted to the amplification curve. The colours represented are dark/purple—ROX dye was added to the well; light/orange—ROX dye was not added to the well, based on a dataset of 13 qLAMP plates corresponding to 2016 well-samples. For this plot, not-called amplification curves ('undetermined') are represented by '200', the maximum number of 18-second isothermal cycles permitted for this qLAMP reaction.

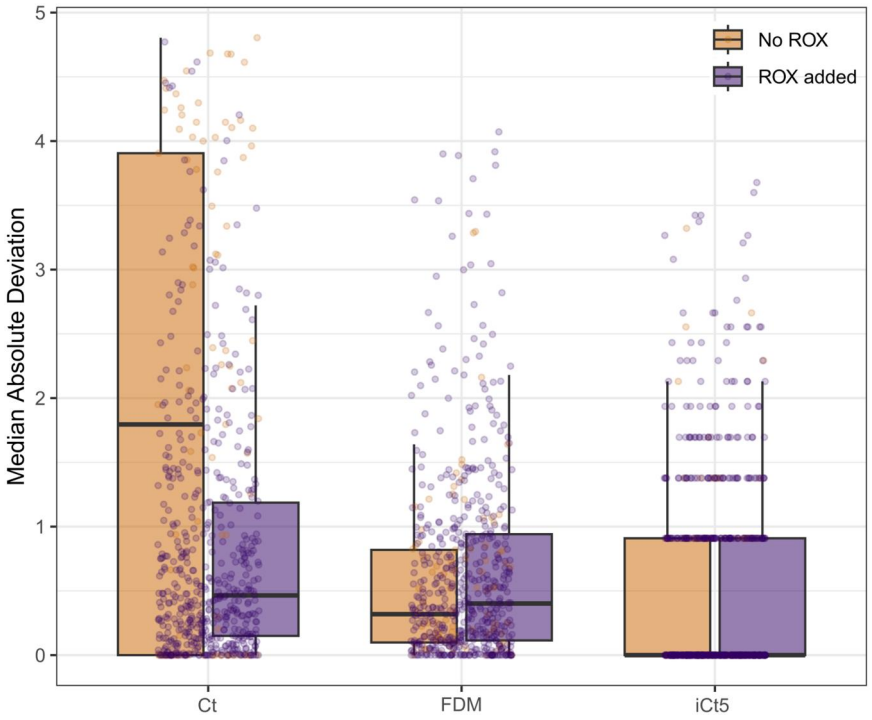

Figure 4 Box-and-jitter plots of within-technical replicate dispersion (MAD—median absolute deviation) of ROX-dye not added (light/orange/left) and ROX-dye added (dark/purple/right) wells. MAD is lowest for the iCT_5 method.

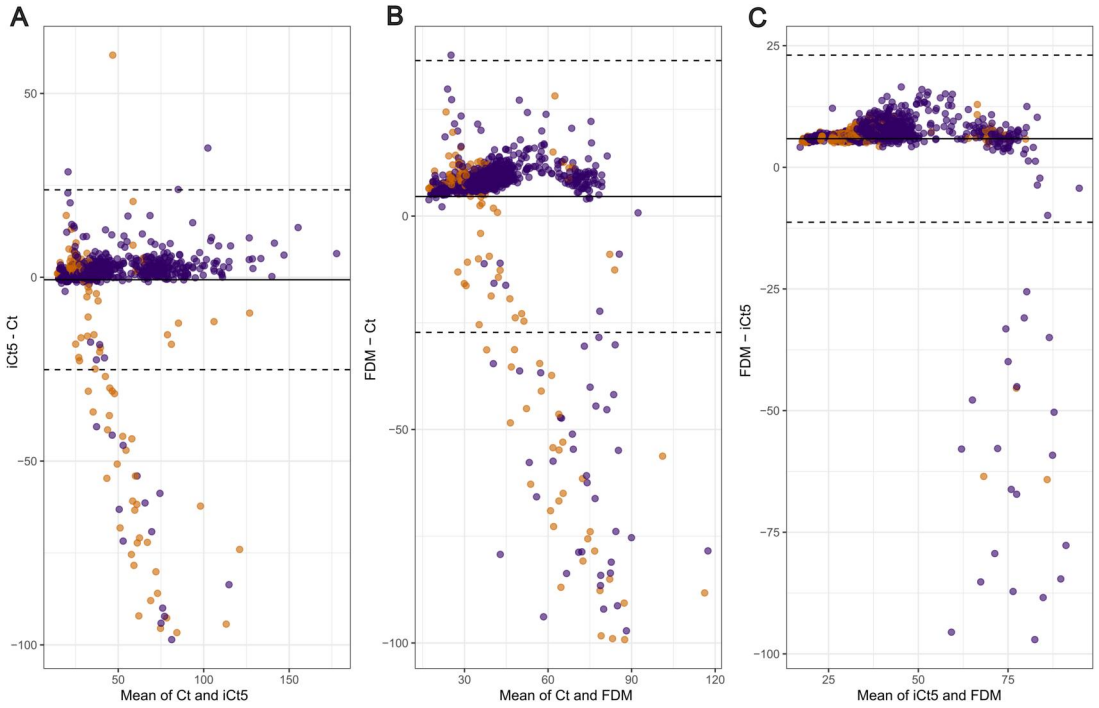

Figure 5 Bland-Altman agreement plots to evaluate the performance of A) iCt_5 to Ct, B) FDM to Ct, and 3) FDM to iCt_5. The horizontal line represents average bias. $y = 0$ represents perfect agreement and the dashed lines represent the 95% limits of agreement. The x-axis denotes the mean of cycles called across both methods. The plot only includes pairwise complete observations; excluding wells where calling failed for either method. The colours represented are dark/purple—ROX dye was added to the reaction; light/orange—ROX dye was not added to the reaction. One outlier of FDM—Ct and FDM—$iCt_5 > 150$ was excluded, respectively.

qPCR reactions to the same degree as the auto-threshold Ct calculated by the StepOne software.

Percentage of successful calls and justification for $n = 5$ cycles for iCt applied to qLAMP

Figure 3 shows a scatter plot matrix for the metrics Ct, iCt_5 ($n = 5$ cycles), iCt_1 ($n = 1$ cycle), iCt_2 ($n = 2$ cycles) as well as FDM. The absence of ROX dye in dataset 1 contributed to variability in Ct values, however, not all Ct variability could be explained by the absence of ROX dye (Fig. 3). FDM and iCt use raw fluorescence curves, so ROX variability did not influence these metrics. Among all methods, iCt_5 had the lowest number of undetermined wells compared to any other method, regardless of ROX status (3.22% in wells without ROX and 7.23% in wells with ROX, Table 3). The highest percentage of undetermined wells without ROX dye was Ct (43.73%) and iCt_1 in plates containing ROX (26.16%). Increasing the forward window from 1 to 5 cycles substantially improved call stability without introducing additional bias, resulting in the lowest rate of undetermined wells across both ROX and non-ROX wells (Table 3).

Within-technical replicate dispersion of successfully called wells across Ct, FDM and iCt5 metrics applied to qLAMP

MAD, comparing agreement of called metrics between groups of technical replicates, showed highest median values in the Ct metric with and without ROX. FDM had lower dispersion values, but MAD in iCt_5 were lowest (Fig. 4). This shows that iCt_5 called the most similar values between technical replicates, which indicates that it performs better than FDM and Ct, regardless of addition of ROX dye to wells. Kruskal–Wallis tests for MAD between metrics were significant for both ROX conditions (ROX added KW-H = 83.05; $P < .001$; without ROX KWH = 38.94, $P < .001$). Pairwise *post hoc* Dunn's tests revealed that regardless of ROX status, MAD of Ct and FDM did not significantly differ from each other, but that MAD of iCt_5 significantly differed from both Ct and FDM metrics ($P < .001$; Supplementary Table 1).

Agreement of successfully called wells across Ct, FDM, and iCt5 metrics applied to qLAMP

The Bland-Altman agreement plots (Fig. 5) revealed that agreement between methods was dependent on amplification timing as well as addition of ROX when determining Ct. For early calls, Ct, iCt_5, and FDM showed closer agreement. In comparisons involving Ct, differences increased progressively with later mean cycle values, indicating proportional bias whereby Ct increasingly reported later amplification relative to both iCt_5 and FDM. This systematic bias in Ct-based comparisons (iCt_5 vs. Ct and FDM vs. Ct) was enriched among non-ROX wells, confirming that absence of ROX normalisation contributes to Ct instability and inflated disagreement in dataset 1.

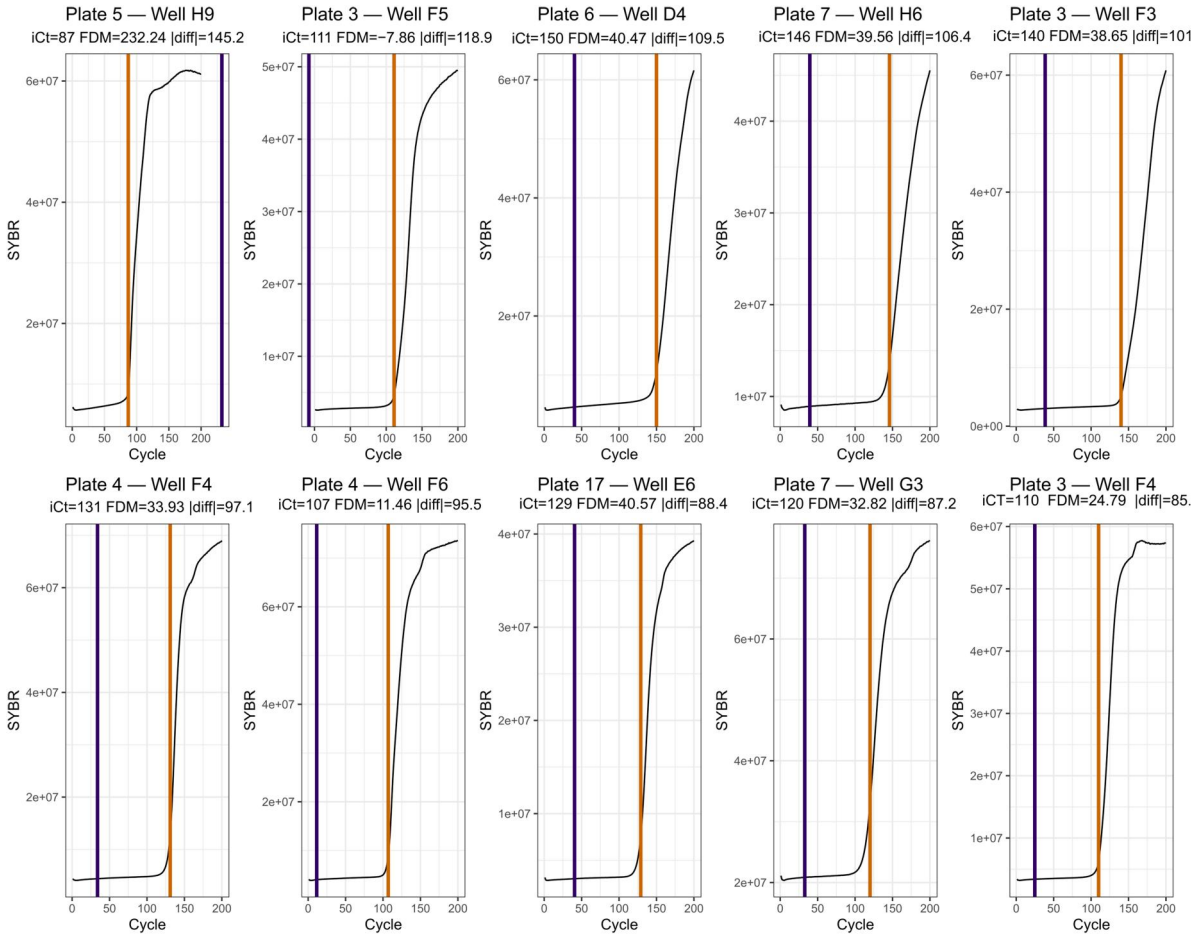

Figure 6 Depiction of the amplification curves of the 10 wells with lowest agreement between iCt_5 (light/orange vertical bar) and FDM (dark/purple vertical bar). 'diff' refers to the numeric difference between iCt_5 and FDM metrics.

This pattern suggests reduced robustness of Ct under late amplification conditions, which is problematic in cases where treatments downregulate genes towards later amplification. Comparison of FDM and iCt_5 as well as Ct show that FDM, due to its nature as a metric derived from a fitted curve rather than from actual fluorescence values, has a curvilinear relationship with both other metrics, which indicates that FDM values are biased towards the time point during the total time window of the reaction at which the amplification is called. Comparison of FDM and iCt_5 further demonstrated that, while both methods agreed closely for early calls, a distinct subset of reactions with higher mean call numbers exhibited substantial negative deviations (FDM—$iCt_5 < 0$). This suggests that assumptions inherent to logistic curve fitting may not universally hold for qLAMP kinetics. In contrast, iCt_5, being derived directly from relative changes in the observed fluorescence signal, does not impose a predefined curve shape and appears less sensitive to such deviations.

The iCT_5 metric identifies the cycle at which the forward 5-cycle fluorescence ratio (signal($t+5$)/signal(t)) is maximal. Importantly, this corresponds to the start of the steepest 5-cycle (or 90 seconds) growth window, not the midpoint of the amplification burst. In contrast, FDM estimates the inflection point of a four-parameter logistic model fitted to the entire amplification curve, which assumes a symmetric sigmoid shape and a well-defined plateau. The 10 wells with largest disagreement between FDM and iCt_5 reveal that most of these wells amplify late in the reaction. Fluorescence increases in all cases are tapering off by cycle 200, as otherwise iCt_5 would have returned an

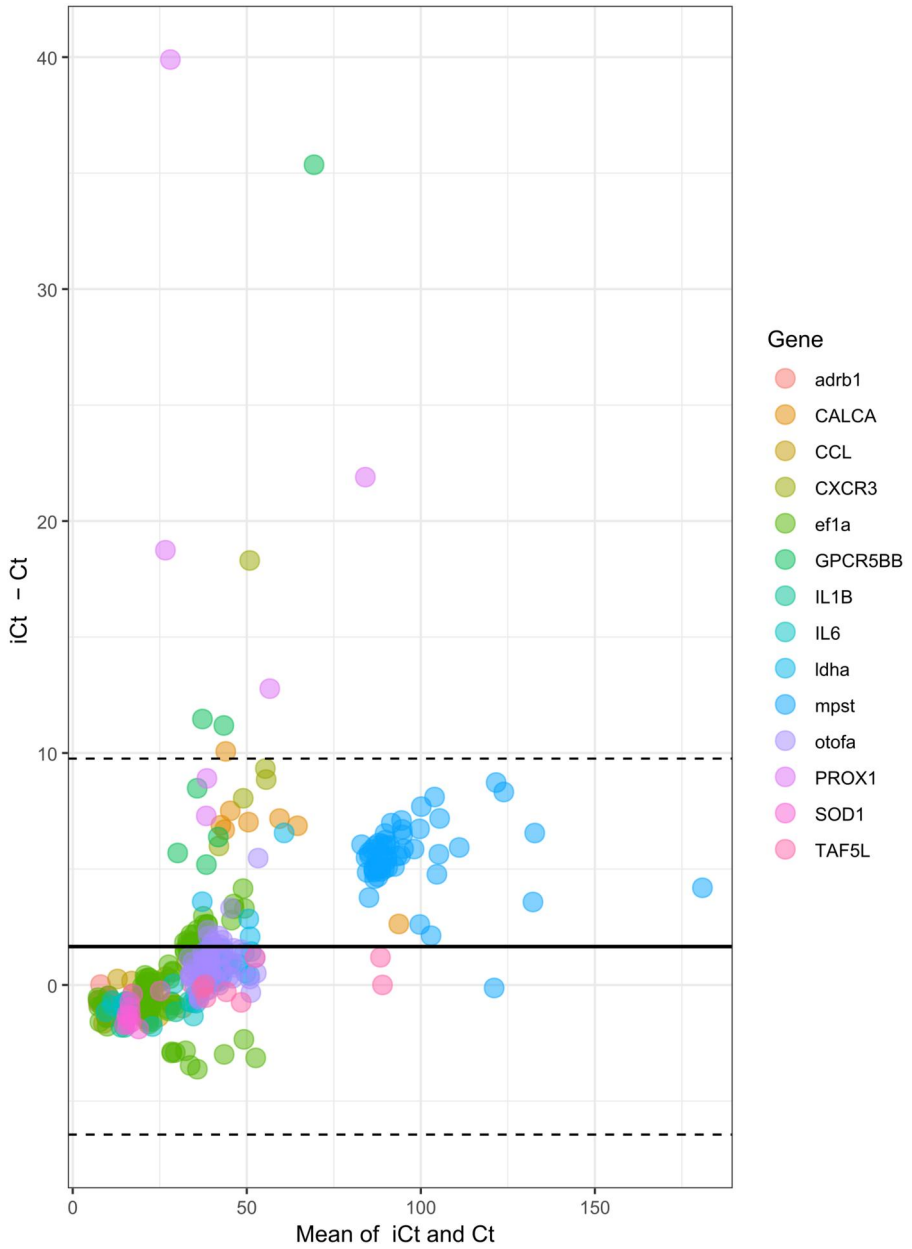

Figure 7 Bland-Altman agreement plot for qLAMP dataset 2, visualising 14 different genes. The horizontal line represents average bias. $y = 0$ represents perfect agreement and the dashed lines represent the 95% confidence interval. The x-axis denotes the mean of cycles called across both methods. The plot only includes pairwise complete observations; excluding wells where calling failed for either method.

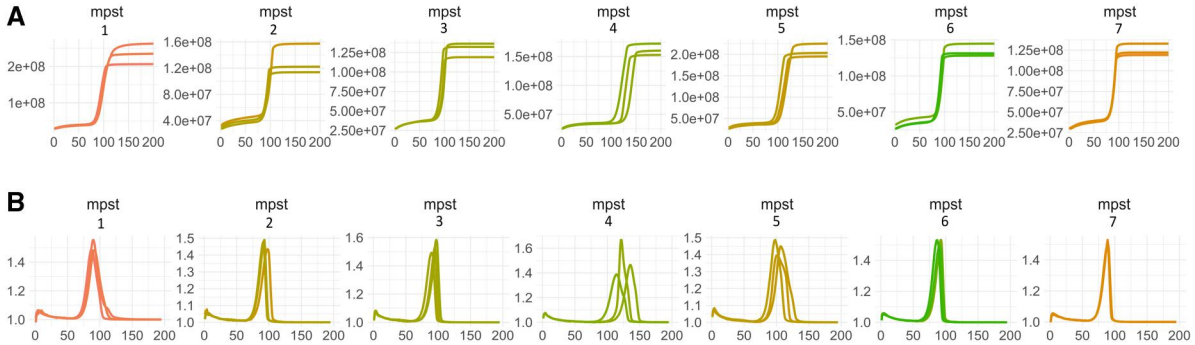

Figure 8 LAMP amplification plots for Ct (A) and iCt (B) for the gene *mpst*. The number above each plot is the biological replicate and each line represents a technical replicate. The absolute fluorescence plots show a steep rise in the fluorescence in the linear phase, which may cross an auto threshold to count as Ct value, before commencement of the exponential phase. *LAMPrey* would however not pick these initial rises in fluorescence as the iCt value (small peak in panel B), and use the maximum peak instead.

Undetermined value. While iCt_5 correctly calls the start of the 5 cycles with highest fluorescence increases, FDM is calling mostly early cycles, presumably due to a failure in curve fitting (Fig. 6). In the case of Plate 5—Well H9, FDM called a very late cycle, possibly due to the reaction curve performing a second, sigmoidal-like increase instead of plateauing (Fig. 6).

LAMPrey can accurately and reliably analyse qLAMP data with lower plate variability

In dataset 2, most wells are in agreement for Ct and iCt_5 in the sense that they lie within the 95% limits of agreement. Outlier values beyond the 95% limits of agreement are likely due to too early calls of Ct. Upon visual inspection, these curves amplify late, do not show pronounced plateaus, and have slower amplification kinetics than expected from an exponential model (Supplementary Fig. 1, see online supplementary material for a colour version of this figure). They are also characteristic of the overall shape of the agreement plot, which shows that iCt_5 has consistently later calls than Ct, indicative of the non-exponential reaction kinetics of qLAMP (Fig. 7), which we showed on dataset 1 to also prevent sigmoidal curve-fitting.

As an example for non-experimental reaction kinetics, qLAMP amplification curves for the gene *mpst* (mercaptopyruvate sulfurtransferase; seven biological replicates from each 20 embryos with three technical replicates each) are shown in Fig. 8. This gene shows a pronounced early linear amplification phase, which may be an explanation for the earlier Ct calls compared with iCt_5 (cf. the blue point cloud in Fig. 7).

Conclusion

In conclusion, we have developed an open-source metric for RNA quantitation that enhances reproducibility and better supports open science. Our LAMPrey set of functions overcomes the bias of LAMP's divergence from exponential amplification kinetics and allows to accurately analyse and interpret qLAMP data, thus further reducing the barrier to entry to this already easily accessible technology. Our approach, based on the iCt, provides a reliable alternative to automatic Ct computation by capturing the start point of the 5-cycle phase of maximal fluorescence increase independently of thermal cycler or software used. This method addresses the two challenges of arbitrary or proprietary threshold setting and the variable initial amplification dynamics in qLAMP reactions, leading to more consistent and comparable results across studies and technologies. We believe that the LAMPrey set of functions are a valuable tool for the research community, facilitating improved and reproducible analysis of qPCR and qLAMP data.

Acknowledgements

We extend our thanks to Victoria Scott and Emma Chapman (University of Hull) for providing some of the LAMP data, and Graham Sellers (University of Hull) for providing the NEB library quantification kit data.

Author contributions

Jiao Li (Data curation [equal], Formal analysis [equal], Investigation [equal], Writing—review & editing [equal]), Sofia Vamos (Data curation [equal], Resources [equal], Writing—review & editing [equal]), Francisco Rivero (Conceptualization [equal], Funding acquisition [equal], Supervision [equal], Writing—review & editing [equal]), and Katharina C. Wollenberg Valero (Conceptualization [equal], Formal analysis [equal], Funding acquisition [equal], Methodology [equal], Supervision [equal], Writing—original draft [equal], Writing—review & editing [equal])

Supplementary material

Supplementary material is available at *Biology Methods and Protocols* online.

Conflicts of interest

None declared.

Funding

K.C.W.V., J.L., and S.V. acknowledge funding by the European Union (ERC, MolStressH2O, #101044202). Views and opinions expressed are however those of the author(s) only and do not necessarily reflect those of the European Union or the European Research Council Executive Agency. Neither the European Union nor the granting authority can be held responsible for them.

Ethics statement

All experiments performed on zebrafish embryos and larvae less than 5dpf were approved by the Ethics committee of the University of Hull (FEC_2019_194 Amendment 1) as well as the Animal Welfare Body of University College Dublin (Arec-E-23-16).

Data availability statement

All scripts and data are available at https://github.com/dodged13/LAMPrey

References

1. Bustin SA, Ruijter JM, van den Hoff MJB *et al.* MIQE 2.0: revision of the Minimum Information for Publication of Quantitative Real-Time PCR Experiments Guidelines. *Clin Chem* 2025;**71**:634–51. https://doi.org/10.1093/clinchem/hvaf043
2. Notomi T, Okayama H, Masubuchi H *et al.* Loop-mediated isothermal amplification of DNA. *Nucleic Acids Res* 2000;**28**:E63. https://doi.org/10.1093/nar/28.12.e63
3. Alves PA, de Oliveira EG, Franco-Luiz APM *et al.* Optimization and clinical validation of colorimetric reverse transcription loop-mediated isothermal amplification, a fast, highly sensitive and specific COVID-19 molecular diagnostic tool that is robust to detect SARS-CoV-2 variants of concern. *Front Microbiol* 2021;**12**:713713. https://doi.org/10.3389/fmicb.2021.713713
4. Kitagawa Y, Orihara Y, Kawamura R *et al.* Evaluation of rapid diagnosis of novel coronavirus disease (COVID-19) using loop-mediated isothermal amplification. *J Clin Virol* 2020;**129**:104446. https://doi.org/10.1016/j.jcv.2020.104446
5. Lee JYH, Best N, McAuley J *et al.* Validation of a single-step, single-tube reverse transcription loop-mediated isothermal amplification assay for rapid detection of SARS-CoV-2 RNA. *J Med Microbiol* 2020;**69**:1169–78. https://doi.org/10.1099/jmm.0.001238
6. Lim B, Ratcliff J, Nawrot DA *et al.* Clinical validation of optimised RT-LAMP for the diagnosis of SARS-CoV-2 infection. *Sci Rep* 2021;**11**:16193. https://doi.org/10.1038/s41598-021-95607-1
7. Mouliou DS, Gourgoulianis KI. False-positive and false-negative COVID-19 cases: respiratory prevention and management strategies, vaccination, and further perspectives. *Expert Rev Respir Med* 2021;**15**:993–1002. https://doi.org/10.1080/17476348.2021.1917389
8. Zhang X, Zhao Y, Zeng Y *et al.* Evolution of the probe-based loop-mediated isothermal amplification (LAMP) assays in pathogen detection. *Diagnostics* 2023;**13**:1530. https://doi.org/10.3390/diagnostics13091530
9. Guescini M, Sisti D, Rocchi MBL *et al.* A new real-time PCR method to overcome significant quantitative inaccuracy due to slight amplification inhibition. *BMC Bioinformatics* 2008;**9**:326. https://doi.org/10.1186/1471-2105-9-326
10. Luu-The V, Paquet N, Calvo E *et al.* Improved real-time RT-PCR method for high-throughput measurements using second derivative calculation and double correction. *BioTechniques* 2005;**38**:287–93. https://doi.org/10.2144/05382RR05
11. Zhang Y, Li H, Shang S *et al.* Evaluation validation of a qPCR curve analysis method and conventional approaches. *BMC Genomics* 2021;**22**:680. https://doi.org/10.1186/s12864-021-07986-4
12. Ritz C, Spiess A-N. *qpcR*: an R package for sigmoidal model selection in quantitative real-time polymerase chain reaction analysis. *Bioinformatics* 2008;**24**:1549–51. https://doi.org/10.1093/bioinformatics/btn227
13. R Core Team. *R: A Language and Environment for Statistical Computing*. Vienna, Austria: R Foundation for Statistical Computing, 2024. https://www.R-project.org/
14. Wickham H. . *Elegant Graphics for Data Analysis*. New York: Springer, 2016. https://ggplot2.tidyverse.org
15. Karthik K, Rathore R, Thomas P, *et al.* Rapid and visual loop mediated isothermal amplification (LAMP) test for the detection of Brucella spp. and its applicability in epidemiology of bovine brucellosis. Veterinarski Arhiv 2016;**86**:35–47. 10.1080/01652176.2014.966172

Biology Methods and Protocols, 2026, 11, 1–10
https://doi.org/10.1093/biomethods/bpag016
Methods Article